

A Novel Algorithm for Rotor Speed Estimation of DFIGs Using Machine Active Power based on MRAS Observer

R. Ajabi-Farshbaf*, M. R. Azizian, V. Yousefzad

Faculty of Electrical Engineering, Sahand University of Technology (SUT), Tabriz, Iran.

Abstract-This paper presents a new algorithm based on Model Reference Adaptive System (MRAS) and its stability analysis for sensorless control of Doubly-Fed Induction Generators (DFIGs). The reference and adjustable models of the suggested observer are based on the active power of the machine. A hysteresis block is used in the structure of the adaptation mechanism, and the stability analysis is performed based on sliding mode conditions. Simulation and practical results show appropriate operation and speed tracking of the observer with regard to obtained stability conditions.

Keyword: Active power; Doubly fed induction generator; MRAS-based observer; Stability analysis.

NOMENCLATURE

General	
R_s	Stator resistance
V, i	Voltage and current
ψ	Stator or rotor flux
σ	leakage coefficient
L, L_s	Stator and leakage inductance
ω_s, ω_r	Stator and rotor electrical frequency
ω_m	Mechanical speed
ω_0	Electrical frequency of the ac mains
L_m	Mutual inductance
T_e	Electromagnetic torque
ρ	Pair of poles
P_s	Active power of stator-side
γ_m	Rotor position
ε_r	Error
γ_{is}	Angle between stator and α_s vectors
Superscripts	
\rightarrow	Vector sign
r	Rotor reference frame
\wedge	Estimation value
*	Conjugate vector
Subscripts	
α, β	Variables on $\alpha\beta$ reference frame
d, q	Variables on dq reference frame
r, s	Stator or rotor quantities

est Estimation value

1. INTRODUCTION

Generally, machine speed data is needed to implement most of control strategies, especially vector control [1]. Tachogenerators, resolvers, incremental and light encoders are common-used speed sensors, which may cause some problems. These sensors reduce system reliability and require accurate installation and calibration, maintenance, extra cabling, and immunizing against electric noises. Furthermore, in some applications, it is difficult to construct speed feedback. Installation and maintenance of speed sensors in wind turbines and generators with high height is a time-consuming and costly act. Therefore, sensor elimination leads to significant facilities. When speed sensors fail, the system controller receives incorrect feedback signals, which disrupts its operation [2].

Many speed estimation strategies are developed and explained in previously reported works. Some of Basic methods are explained in [3] for induction machines. Speed estimation algorithms for Doubly-Fed Induction Machines (DFIMs) and DFIGs are generally developed forms of basic algorithms. Speed estimation algorithms for Doubly-Fed Induction Machines (DFIMs) and DFIGs are generally developed forms of basic algorithms. Especially in DFIG, rotor-side parameters are measurable and therefore they can be used in the estimation algorithms. Some of basic methods are classified as follows:

MRAS based algorithms; in [4] basic structure of MRAS is changed to be applied in DFIG where a new adaptation

Received: 25 Mar. 2016

Revised: 03 Apr. 2017 and 25 Jul. 2017

Accepted: 19 Oct. 2017

*Corresponding author:

E-mail: r_ajabi@sut.ac.ir (R. Ajabi-FARshbaf)

Digital object identifier: 10.22098/joape.2018.2132.1200

mechanism and new state variables are selected. Four MRAS-based observers are evaluated in [5] for DFIGs, State variables of the proposed observers are different. In [6], another MRAS observer is introduced for DFIMs where its main specification is direct estimation of torque and rotor flux components. The suggested MRAS algorithm in [7], applies a constant gain in the adjustable model of the MRAS which solves drift problems of integrators. In [8] a MRAS algorithm is developed which is based on neural networks. In the MRAS observer proposed in [9], machine reactive power is used as a new adaptation mechanism. In [10], air-gap electromotive force (EMF) is defined as the working variable and MRAS control strategy is considered to calculate the rotor position.

Adaptive observers; in [11], an adaptive observer, which is an extension of the basic Luenberger algorithm, is designed for sensorless control of DFIGs. A reduced-order adaptive observer is explained in [12] for stator flux and speed estimation. Structure of the conventional Kalman filter is changed in [13] to be used for sensorless control of DFIM. Rotor side measurements is also applied in the proposed algorithm. In [14], another reduced-order adaptive observer is presented for DFIG. It is also based on Luenberger observer and contains different state variables.

Other methods; A straightforward algorithm is designed in [15] for rotor position estimation, in which flux calculations and integrators not included. Speed estimation from machine slip is explained in [16]. In [17], a sensorless control strategy is developed which is based on the Phase-Locked Loop (PLL) system. According to the authors' discussion, it is independent of machine parameters. The presented algorithm in [18] is relatively simple and contains no flux calculations. Undesired effects of integrators is reduced in [18] which is its main advantage.

According to the numerous works reported in the literature, MRAS based observers have proved to provide more acceptable operation, especially with the state variable, which is independent from machine fluxes. Based on reported works evaluation, an adaptive observer consists of system model, adaptation mechanism, a term for model correction and stability analysis. In all reported works one or more of these parts have designed with a new procedure. Therefore, in this paper, a new MRAS based speed estimation algorithm is introduced. Compared with previously reported works in this paper a hysteresis block is used in the structure of the adaptation mechanism, and the stability analysis is

performed based on sliding mode conditions. Purposed method stability and parameter sensitivity is analysed with extensive formulation. Active power of the machine is considered as state variable of the proposed method and a new adaptation mechanism is extracted. Therefore, the proposed method in this paper is a completely new algorithm and its equations is exclusive to suggested model because:

- 1- It is based on DFIG active power.
- 2- The suggested adaptation mechanism is based on a hysteresis block.
- 3- Stability study is performed based on operation of the hysteresis controller and sliding mode conditions.

Since the proposed method is based on hysteresis analysis, it has simple concepts to understand. Therefore, simplicity of the proposed method is its main advantage over previous works.

Consequently, the proposed MRAS is unique. This paper is organized as follows. In Section 2, the dynamic model of DFIG is presented. The proposed observer structure is described in Section 3. Section 4 presents stability analysis of the suggested MRAS-based speed estimation algorithm. Simulation and practical results are presented in sections 5 and 6, respectively. Finally, conclusions are included in Section 7.

2. DYNAMIC MODELLING OF DFIG

Figure. 1 shows the equivalent circuit of a DFIG in the $\alpha\beta$ frame. Assuming $\alpha\beta$ fluxes as state variables, the basic equations of a DFIG can be written as follows [19]:

$$\frac{d}{dt} \begin{bmatrix} \psi_{\alpha s} \\ \psi_{\beta s} \\ \psi_{\alpha r} \\ \psi_{\beta r} \end{bmatrix} = \begin{bmatrix} \frac{-R_s}{\sigma L_s} & 0 & \frac{R_s L_m}{\sigma L_s L_r} & 0 \\ 0 & \frac{-R_s}{\sigma L_s} & 0 & \frac{R_s L_m}{\sigma L_s L_r} \\ \frac{R_r L_m}{\sigma L_s L_r} & 0 & \frac{-R_r}{\sigma L_r} & -\omega_m \\ 0 & \frac{R_r L_m}{\sigma L_s L_r} & \omega_m & \frac{-R_r}{\sigma L_r} \end{bmatrix} \begin{bmatrix} \psi_{\alpha s} \\ \psi_{\beta s} \\ \psi_{\alpha r} \\ \psi_{\beta r} \end{bmatrix} + \begin{bmatrix} V_{\alpha s} \\ V_{\beta s} \\ V_{\alpha r} \\ V_{\beta r} \end{bmatrix} \quad (1)$$

where σ is leakage coefficient equals $1 - \frac{L_m^2}{L_s L_r}$ and current and flux relations are as follows:

$$\begin{bmatrix} \psi_{\alpha s} \\ \psi_{\beta s} \end{bmatrix} = \begin{bmatrix} L_s & 0 \\ 0 & L_s \end{bmatrix} \cdot \begin{bmatrix} i_{\alpha s} \\ i_{\beta s} \end{bmatrix} + \begin{bmatrix} L_m & 0 \\ 0 & L_m \end{bmatrix} \cdot \begin{bmatrix} i_{\alpha r} \\ i_{\beta r} \end{bmatrix} \quad (2)$$

$$\begin{bmatrix} \psi_{\alpha r} \\ \psi_{\beta r} \end{bmatrix} = \begin{bmatrix} L_m & 0 \\ 0 & L_m \end{bmatrix} \cdot \begin{bmatrix} i_{\alpha s} \\ i_{\beta s} \end{bmatrix} + \begin{bmatrix} L_r & 0 \\ 0 & L_r \end{bmatrix} \cdot \begin{bmatrix} i_{\alpha r} \\ i_{\beta r} \end{bmatrix} \quad (3)$$

Furthermore, the electrical torque equation of DFIG is as follows:

$$T_e = \frac{3}{2} L_m \rho \operatorname{Im} \left\{ \begin{matrix} \vec{i}_s \\ \vec{i}_r \end{matrix} \right\} \quad (4)$$

where ρ is the machine pole pairs. Considering L_{σ} and L_m as leakage and magnetic inductances, respectively, the stator and rotor inductances can be assumed as:

$$\begin{cases} L_s = L_{\sigma s} + L_m \\ L_r = L_{\sigma r} + L_m \end{cases} \quad (5)$$

On the other hand, the relation between machine stator and rotor electric speed is described as:

$$\omega_r + \omega_m = \omega_s \quad (6)$$

A more detailed model of DFIG is explained in [19].

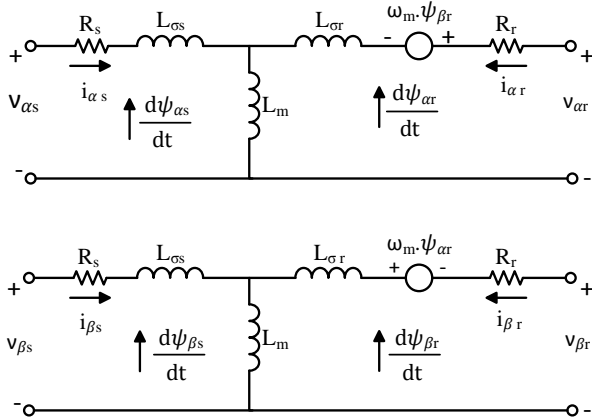


Fig. 1. $\alpha\beta$ model of the DFIG in stator coordinates [19].

3. DESCRIPTION OF OBSERVER STRUCTURE

The suggested MRAS based speed observer is introduced and described in this section. It is well-known that any MRAS based observer consists of three main blocks: reference model, adjustable model, and adaptation mechanism [20]. Fig. 2 depicts a general block diagram of the proposed algorithm. Active power is applied in the equations of reference and adjustable models. The adjustable model is extracted in a way that includes speed as a parameter.

By rewriting (2), we have,

$$\begin{cases} \psi_{\alpha s} = L_s i_{\alpha s} + L_m i_{\alpha r}^s \\ \psi_{\beta s} = L_s i_{\beta s} + L_m i_{\beta r}^s \end{cases} \quad (7)$$

From Eq. (7), stator current components can be obtained as follows:

$$\begin{cases} i_{\alpha s} = \frac{\psi_{\alpha s} - L_m i_{\alpha r}^s}{L_s} \\ i_{\beta s} = \frac{\psi_{\beta s} - L_m i_{\beta r}^s}{L_s} \end{cases} \quad (8)$$

Superscript ‘‘s’’ indicates the parameters that are in the stator frame. The transfer matrix from rotor frame to stator frame is as follows:

$$\begin{bmatrix} i_{\alpha r}^s \\ i_{\beta r}^s \end{bmatrix} = \begin{bmatrix} \cos \gamma_m & -\sin \gamma_m \\ \sin \gamma_m & \cos \gamma_m \end{bmatrix} \begin{bmatrix} i_{\alpha r} \\ i_{\beta r} \end{bmatrix} \quad (9)$$

The transfer function of Eq. (9) depends on the rotor position. Furthermore, the active power of DFIG at the stator-side can be considered as [19]:

$$P_s = \frac{3}{2} \operatorname{Re} \left\{ \vec{V}_s \cdot \vec{I}_s^* \right\} = \frac{3}{2} (V_{\alpha s} i_{\alpha s} + V_{\beta s} i_{\beta s}) \quad (10)$$

Equation (10) is considered as the reference model of the MRAS based observer. By replacing Eq. (8) into Eq. (10) and after simplification, we have,

$$P_{est} = \frac{3}{2L_s} \left\{ V_{\alpha s} \psi_{\alpha s} + V_{\beta s} \psi_{\beta s} - L_m V_{\alpha s} i_{\alpha r}^s - L_m V_{\beta s} i_{\beta r}^s \right\} \quad (11)$$

Stator flux components of Eq. (11) can be obtained as follows:

$$\begin{cases} \psi_{\alpha s} = \int (V_{\alpha s} - R_s i_{\alpha s}) dt \\ \psi_{\beta s} = \int (V_{\beta s} - R_s i_{\beta s}) dt \end{cases} \quad (12)$$

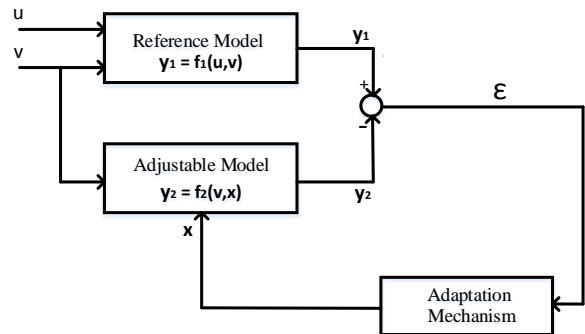


Fig. 2. Basic structure of MRAS.

Equation (11) is considered as the adjustable model of the proposed algorithm. The main block diagram of the introduced MRAS based observer is shown in Fig. 3. The calculated error between reference and estimated active powers is passed through a hysteresis controller block to give estimated speed and then a PI block to give the estimated rotor position.

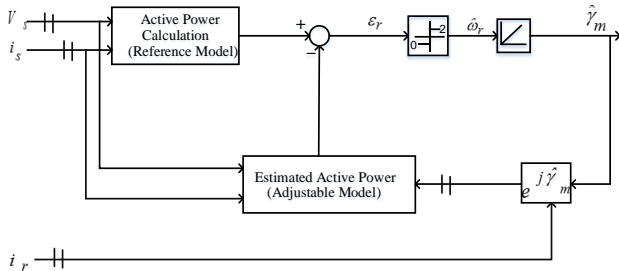


Fig. 3. Proposed structure of active power based MRAS observer.

4. STABILITY ANALYSIS

In this section, a small signal model of the proposed MRAS observer is extracted for stability analysis. It is assumed that a small signal disturbance is given to the system in any stable operating point. It is expected that the overall system is to be stable. The adjustable model of the proposed algorithm can be rewritten as follows:

$$P_{est} = \frac{3}{2L_s} \left\{ \vec{V}_s \vec{\psi}_s - L_m \operatorname{Re} \left[\vec{V}_s \left(i_r e^{j\hat{\gamma}_m} \right)^* \right] \right\} \quad (13)$$

If $\hat{\gamma}_m$ is considered as real value, P_{est} can be considered as P_s . Therefore,

$$P_s = \frac{3}{2L_s} \left\{ \vec{V}_s \vec{\psi}_s - L_m \operatorname{Re} \left[\vec{V}_s \left(i_r e^{j\gamma_m} \right)^* \right] \right\} \quad (14)$$

The established error, \mathcal{E}_r , is then as follows:

$$\mathcal{E}_r = P_s - P_{est} = \Delta P \quad (15)$$

In Fig. 4. phasor diagram of the small signal model is illustrated.

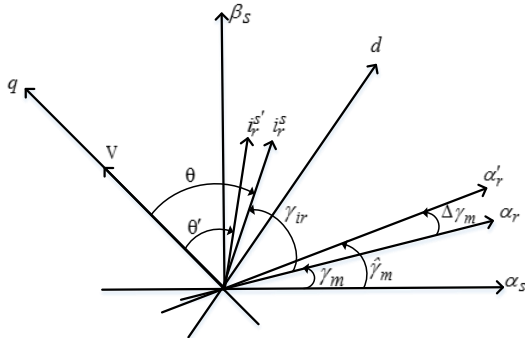


Fig. 4. Phasor diagram of the small signal model.

It is obvious from Eqs. (13) and (14), linearization of Eq. (13) in the steady state conditions, leads to ΔP which is equal to \mathcal{E}_r . Since $|i_r^s| = |i_r|$ and using Fig. 4, we have,

$$\mathcal{E}_r = \Delta P = \frac{-3L_m}{2L_s} |V_s| |i_r^s| \cos \theta = \frac{-3L_m}{2L_s} |V_s| |i_r| \cos \theta \quad (16)$$

$$\mathcal{E}_r = \frac{3L_m}{2L_s} |V_s| |i_r| \sin \theta \Delta \theta \quad (17)$$

In the steady state conditions \mathcal{E}_r is a function of inner product of \vec{V}_s and \vec{i}_r^s , where θ is the angle difference between those vectors. From Fig. 4, we have,

$$\Delta \gamma_m = \hat{\gamma}_m - \gamma_m = \theta' - \theta \quad (18)$$

Therefore,

$$\mathcal{E}_r = \frac{3L_m}{2L_s} |V_s| |i_r| \sin \theta \Delta \gamma_m \quad (19)$$

Using Eq. (18) and Fig. 3, small signal block diagram for stability analysis is illustrated in Fig. 5.

Since, the speed range of the DFIG is usually set to [0.7, 1.3] p.u. [19], in order to establish the appropriate speed range of the estimator, the output of the hysteresis comparator is set to $[0, 2\omega_0]$ p.u. [21, 22], where ω_0 is the electrical frequency of the mains. For correct operation, the selected bandwidth for hysteresis block must be larger than the values of speed range of DFIG. Therefore, the nearest integers are chosen as hysteresis bandwidths. Also, in Fig. 5, T_s is the sampling time.

Stability analysis is based on the sliding mode conditions, in which a system is stable when the product of error (\mathcal{E}_r) and error derivate ($\frac{d\mathcal{E}_r}{dt}$) leads to a negative result. Using Fig. 5 the following relation can be extracted:

$$\frac{d\mathcal{E}_r}{dt} = \frac{3L_m}{2L_s} |V_s| |i_r| \sin \theta \omega_0 (u - \omega_m) \quad (20)$$

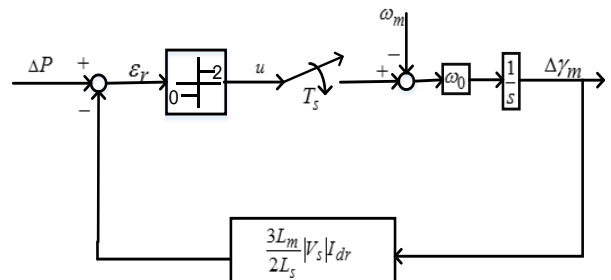


Fig. 5. Block diagram of the small signal model using hysteresis controller for stability analysis.

In Fig. 5, u is the output signal of the hysteresis block. As it mentioned previously, according to hysteresis block output, which is 0 or 2, we have,

$$\begin{cases} \varepsilon_r < 0 \rightarrow u = 0 \rightarrow \\ \frac{d\varepsilon_r}{dt} = \frac{3L_m}{2L_s} |V_s| |i_r| \cdot \sin \theta \cdot \omega_0 (0 - \omega_m) \\ \varepsilon_r > 0 \rightarrow u = 2 \rightarrow \\ \frac{d\varepsilon_r}{dt} = \frac{3L_m}{2L_s} |V_s| |i_r| \cdot \sin \theta \cdot \omega_0 (2 - \omega_m) \end{cases} \quad (21)$$

Finally, from Eq. (21) the stability condition can be defined as Eq. (22) in every operating point.

$$|V_s| \neq 0, \quad \sin \theta < 0 \quad (22)$$

It can be concluded from Eq. (21) and Fig. 4 that \vec{i}_r^s must be lag due to \vec{V}_s , for stable operation of proposed observer.

5. SIMULATION RESULTS

Speed tracking of the proposed method is confirmed by simulation results, which is presented in this section. A 1.5 MW DFIG is simulated using MATLAB/Simulink

software and its parameters are presented in the Appendix. Fig. 6 shows speed tracking capability of the MRAS-based observer where wind speed changes from 15 to 9 m/s. Fig. 7 illustrates speed tracking of the observer at the sub-synchronous condition where wind speed changes from 15 to 6 m/s. As can be seen, the produced error of the suggested speed estimation algorithm is less than 0.05 p.u.

Moreover, to confirm stability condition (21), the angle between \vec{V}_s and \vec{i}_r^s is shown in Fig. 8. It can be proved that $\sin \theta < 0$ is valid for all simulated states.

6. PRACTICAL RESULTS

A laboratory setup is applied to prove some dynamic behaviours of the proposed algorithm. It consists of a wound rotor induction machine (WRIM) connected to the back-to-back converters. Also, a DC motor is coupled mechanically to the WRIM to play the role of a wind turbine. A digital 16-bit dspIC30F4011 controller is used to generate adequate switching signals of the IGBTs [23]. Furthermore, PCI-1716 and PCLD-8710 I/O boards are used for real-time evaluation of the proposed method.

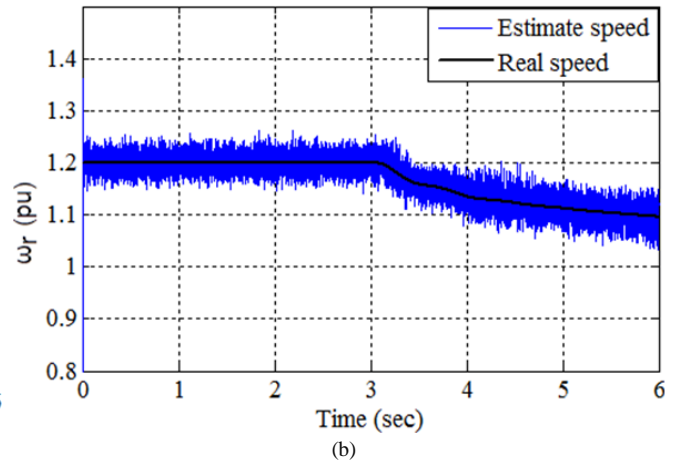
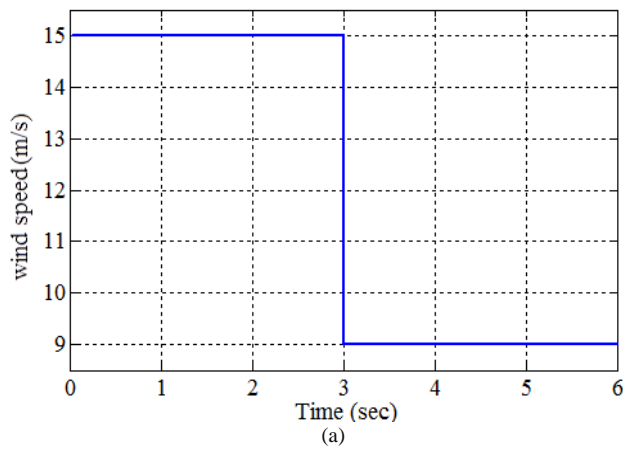


Fig. 6. Speed tracking capability of proposed MRAS-based observer a) wind speed b) real and estimated speed.

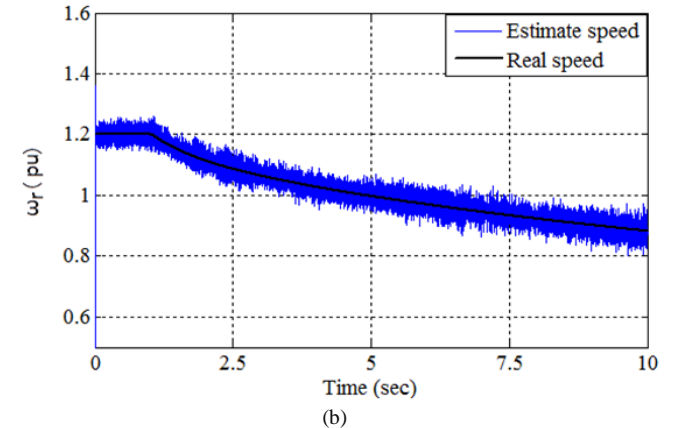
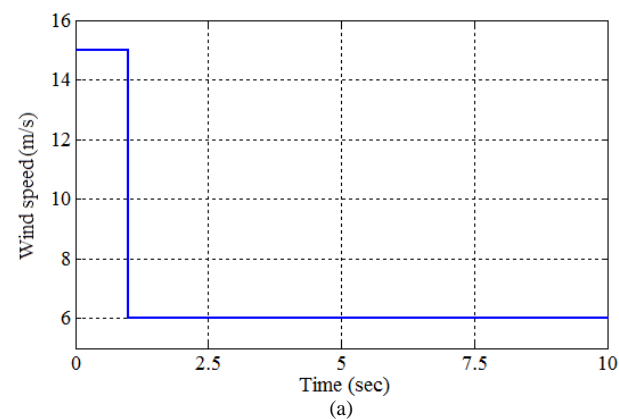


Fig. 7. Speed tracking capability of proposed MRAS-based observer in the sub-synchronous mode a) wind speed b) real and estimated speed.

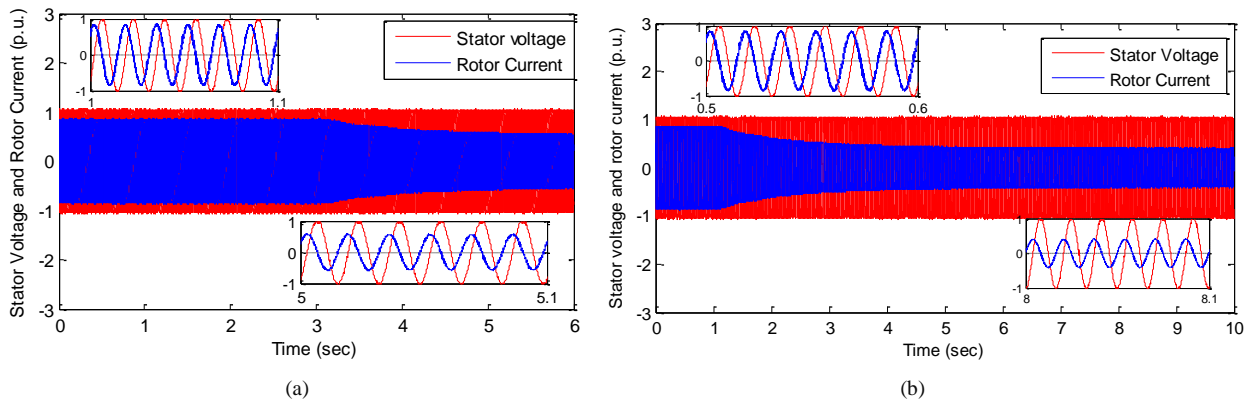


Fig. 8. Stability confirmation of the proposed speed estimation method where wind speed varies a) from 15 to 9 m/s and b) from 15 to 6 m/s.

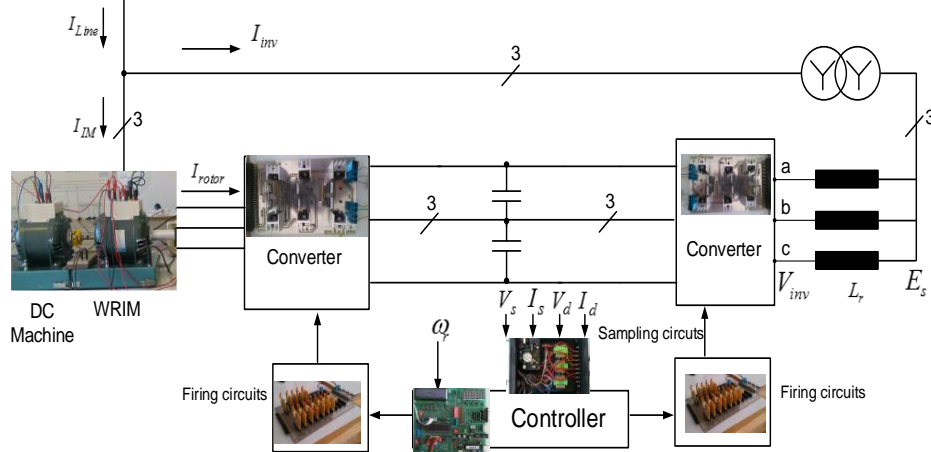


Fig. 9. Laboratory setup.

A brushless DC (BLDC) machine is adjusted and used as a speed sensor. It is coupled to the WRIM and works as a generator. The output voltage of the BLDC is relative with its speed. The IM parameters are presented in the Appendix and Fig. 9 shows the general block diagram of the experimental setup.

machine speed is fixed at 3000 rpm. The rotor current of the IM is also illustrated in the same figure. Speed tracking of the observer is depicted in Fig. 11 where speed changes from 3050 to 3500 rpm, and vice versa. The speed tracking capability of the observer in practical conditions is also acceptable.

Fig. 10 shows steady state operation of the IM where

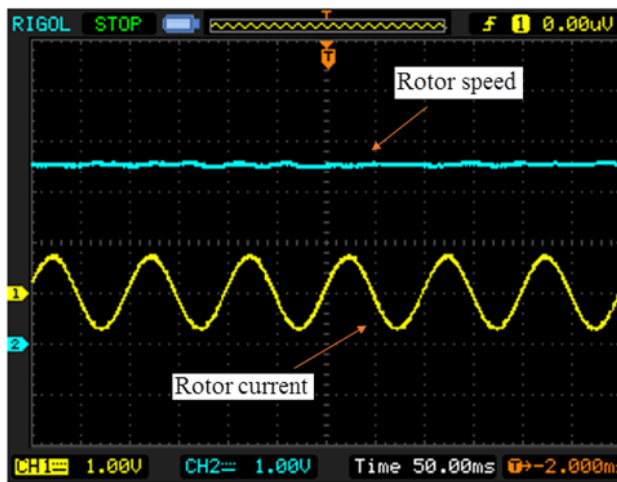


Fig. 10. Rotor current and speed at the steady-state (CH1: 1A/div. CH2: 1000rpm/div.).

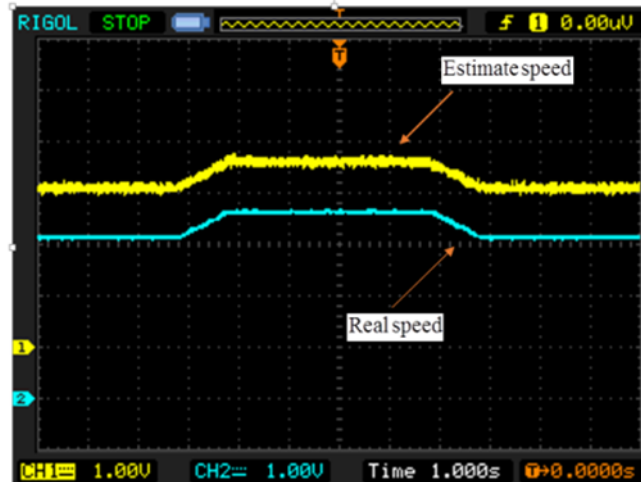


Fig. 11. Speed tracking capability of the proposed method (CH1 & CH2: 1000rpm/div.).

7. CONCLUSIONS

A novel MRAS-based observer is described in this paper. Active power of DFIG is selected as state variable in the structure of the proposed observer. In the adjustable model of the observer, stator currents are transformed to the rotor frame to reveal rotor speed in its formulation. The suggested adaptation mechanism is based on a hysteresis block. The formulation of the MRAS observer in this paper, is unique. Stability of the observer is analysed on the basis of sliding-mode conditions, in detail. The enhanced stability condition is confirmed in the simulation studies. Simulation and practical results show the stable and effective operation of the suggested MRAS-based observer, particularly at the speed tracking. Simulations are performed using MATLAB/Simulink software and practical results are obtained using a DSPIC based microprocessor and a WRIM.

Appendix A.

Table 1. Parameters of the simulated DFIG

Nominal Power	1.5 MW
Nominal Voltage	575 V
Frequency	60 Hz
R_s	0.023 pu
L_{is}	0.18 p.u
R_r	0.016 pu
L_r	0.16 pu
L_m	2.9 pu
Pairs of poles	3
Moment of inertia	0.685 Kg.m ²

Table 2. Parameters of the DFIG, used for practical results

Nominal Power	0.25 kW
Nominal Voltage	120 V
Frequency	50 Hz
R_s	1.7 Ω
L_{is}	0.012 H
R_r	1.6 Ω
L_r	0.012 H
L_m	0.379 H
Pairs of poles	1
Moment of inertia	0.03 Kg.m ²

REFERENCES

- [1] A. Nafar, G. R. Arab Markadeh, A. Elahi, R. Pouraghababa. "Low voltage ride through enhancement based on improved direct power control of dfig under unbalanced and harmonically distorted grid voltage," *J. Oper. Autom. Power Eng.*, vol. 4, no. 1, pp. 16-28, 2016.
- [2] W. Zhong, L. Guo-jie, S. Yuanzhang, and B. T. Ooi, "Effect of erroneous position measurements in vector-controlled doubly fed induction generator," *IEEE Trans. Energy Convers.*, vol. 25, no. 11, pp. 59-69, 2010.
- [3] P. Vas, *Sensorless Vector and Direct Torque Control*. Oxford University Press, 1998.
- [4] R. Cardenas, R. Pena, J. Proboste, G. Asher, J. Clare, "MRAS observer for sensorless control of standalone doubly fed induction generators," *IEEE Trans. Energy Convers.*, vol. 20, no. 4, pp. 710-718, 2005.
- [5] R. Cardenas, R. Pena, J. Clare, G. Asher, J. Proboste, "MRAS observers for sensorless control of doubly-fed induction generators," *IEEE Trans. Power Electr.*, vol. 23, no. 3, pp. 1075-1084, 2008.
- [6] F. C. Dezza, G. Foglia, M. F. Iacchetti, R. Perini, "An MRAS observer for sensorless dfim drives with direct estimation of the torque and flux rotor current components," *IEEE Trans. Power Electr.*, vol. 27, no. 5, pp. 2576-2584, 2012.
- [7] M. Iacchetti, M. S. Carmeli, F. Castelli Dezza, R. Perini, "A speed sensorless control based on a MRAS applied to a double fed induction machine drive," *Electr. Eng.*, vol. 91, no. 6, pp. 337-345, 2010.
- [8] J. A. Cortajarena, J. De Marcos, "Neural network model reference adaptive system speed estimation for sensorless control of a doubly fed induction generator," *Electr. Power Comp. Syst.*, vol. 41, no. 12, pp. 1146-1158, 2013.
- [9] M. P. Pattnaik and D. K. Kastha, "Adaptive speed observer for a stand-alone doubly fed induction generator feeding nonlinear and unbalanced loads," *IEEE Trans. Energy Convers.*, vol. 27, no. 4, pp. 1018-1026, 2012.
- [10] P. K. Gayen, D. Chatterjee, S. K. Goswami, "Stator side active and reactive power control with improved rotor position and speed estimator of a grid connected DFIG (doubly-fed induction generator)," *Energy*, vol. 89, pp. 461-472, 2015.
- [11] D. G. Forchetti, G. O. Garcia, M. I. Valla, "Adaptive observer for sensorless control of stand-alone doubly fed induction generator," *IEEE Trans. Ind. Elect.*, vol. 56, no. 10, pp. 4174-4180, 2009.
- [12] H. Yongsu, K. Sungmin, and H. Jung-Ik, "Sensorless vector control of doubly fed induction machine using a reduced order observer estimating," *In Proc. of the IEEE Energy Convers. Cong. Expo.*, pp. 2623-2630, 2012.
- [13] H. Serhoud, D. Benattous, "Sensorless optimal power control of brushless doubly-fed machine in wind power generator based on extended Kalman filter," *Int. J. Syst. Ass. Eng. Manage.*, vol. 4, no. 1, pp. 57-66, 2013.
- [14] Y. Sheng, V. Ajjarapu, "A speed-adaptive reduced-order observer for sensorless vector control of doubly fed induction generator-based variable-speed wind turbines," *IEEE Trans. Energy Convers.*, vol. 25, no.3, pp. 891-900, 2010.
- [15] A. Karthikeyan, C. Nagamani, G. S. Ilango, "A versatile rotor position computation algorithm for the power control of a grid-connected doubly fed induction generator," *IEEE Trans. Energy Convers.*, vol. 27, no.3, pp. 697-706, 2012.
- [16] G. D. Marques, D. M. Sousa, "Sensorless direct slip position estimator of a DFIM based on the air gap pq - sensitivity study," *IEEE Trans. Ind. Elect.*, vol. 60, no.6, pp. 2442-2450, 2013.
- [17] F. Akel, T. Ghennam, E. M. Berkouk, M. Laour, "An improved sensorless decoupled power control scheme of grid connected variable speed wind turbine generator," *Energy Convers. Manage.*, vol. 78, pp. 584-594, 2014.
- [18] A. Karthikeyan, C. Nagamani, A. B. R. Chaudhury, G. S. Ilango, "Implicit position and speed estimation algorithm without the flux computation for the rotor side control of

- doubly fed induction motor drive,” *IET Electr. Power Appl.*, vol. 6, no. 4, pp. 243-252, 2012.
- [19] G. Abad, J. López, M. A. Rodríguez, L. Marroyo, G. Iwanski, “Dynamic modeling of the doubly fed induction machine,” doubly fed induction machine: modeling and control for wind energy generation, pp. 209-239, 2011.
- [20] S. Maiti, C. Chakraborty, “MRAS-based speed estimation techniques for vector controlled double inverter-fed slipring induction motor drive,” *Proc. 34th Ann. Conf. IEEE Ind. Elect.*, pp. 1275-1280, 2008.
- [21] G. D. Marques, D. M. Sousa, “New sensorless rotor position estimator of a DFIG based on torque Calculations-Stability study,” *IEEE Trans. Energy Convers.*, vol. 27, no. 1, pp. 196-203, 2012
- [22] G. D. Marques, D. Mesquita e Sousa, “A new sensorless MRAS based on active power calculations for rotor position estimation of a DFIG,” *Adv. Power Electr.*, vol. 2011, pp. 1-8, 2011.
- [23] A. Mokhberdoran, A. Ajami, “Symmetric and asymmetric design and implementation of new cascaded multilevel inverter topology,” *IEEE Trans. Power Electr.*, vol. 29, no.11, pp. 6712-6724, 2014.